

Optimal SKA Dish Configuration using Genetic Algorithms

Adam Gauci¹, Kristian Zarb Adami², John Abela³, Babak E. Cohanim⁴

¹*Department of Intelligent Computer Systems, Faculty of ICT, University of Malta, Malta.*

²*Department of Physics, Faculty of Science, University of Malta, Malta.*

³*Department of Computer Information Systems, Faculty of ICT, University of Malta, Malta.*

⁴*Mission Design Group Leader, Draper Laboratory, 555 Technology Square, Cambridge MA 02139.*

Released 2011 Xxxxx XX

ABSTRACT

The Square Kilometre Array (SKA) is a radio telescope designed to operate between 70MHz and 10GHz. Due to this large bandwidth, the SKA will be built out of different collectors, namely antennas and dishes to cover the frequency range adequately. In order to deal with this bandwidth, innovative feeds and detectors must be designed and introduced in the initial phases of development. Moreover, the required level of resolution may only be achieved through a groundbreaking configuration of dishes and antennas. Due to the large collecting area and the specifications required for the SKA to deliver the promised science, the configuration of the dishes and the antennas within stations is an important question. This research builds on the work done before by Cohanim et al. (2004), Hassan et al. (2005) and Grigorescu et al. (2009) to further investigate the applicability of machine learning techniques to determine the optimum configurations for the collecting elements within the SKA. This work primarily uses genetic algorithms to search a large space of optimum layouts. Every genetic step provides a population with candidate individuals each of which encodes a possible solution. These are randomly generated or created through the combination of previous encodings. In this study, a number of fitness functions that rank individuals within a population of dish configurations are investigated. The UV density, connecting wire length and power spectra are considered to determine a good dish layout.

Key words: SKA, radio telescope, machine learning, evolutionary programming, genetic algorithms

1 INTRODUCTION

The SKA will be an instrument through which major scientific discoveries are to be made. Although the construction will follow a phased approach, phase 1 of the SKA is already a formidable instrument and will undoubtedly shed light on the evolutionary stages of the universe from the epoch of reionisation as well as improve our understanding of gravity through the detection of binary and millisecond pulsars (Garrett et al. 2010).

Dishes and antenna arrays will, using state of the art receivers, provide unprecedented sensitivity between 70MHz and 10GHz (Garrett et al. 2010). The required resolving power unavoidably dictates an enormous spatial extent ($\approx 3000\text{km}$) in the initial phase and will cost around 500M Euro (Dewdney 2010). A pioneering design minimising infrastructure, networking and other costs whilst still achieving the

desired specifications is of importance both in the construction phase, but more importantly in the maintenance and running costs of the telescope. Grigorescu et al. (2009) estimate that 100M Euro will most likely be allocated to cabling and trenching that connects the stations together.

In this study, the applicability of Genetic Algorithms (GA) to determine the most optimum configurations for the dish array is investigated. Such evolutionary programming approaches are based on Darwin's theory of natural selection in which the fittest individuals from each population survive and generate offspring chromosomes that encode configurations which are closer to the optimum solution. In Section 2, an introduction to GAs is presented while in Section 3, the work done for dish array optimisation is discussed. Following details on the implemented genetic operators and fitness functions, various cases together with the obtained results

are presented in Section 4 and Section 5. Some conclusions are drawn in Section 6.

2 GENETIC ALGORITHMS

Genetic Algorithms (GAs) are search heuristics that follow the natural process of evolution to determine the most fit hypothesis from a pool of possible solutions. Unlike other search techniques that adopt a brute-force or iterative strategy, GAs combine parts of the best know solutions to try and create better encodings. This evolutionary programming methodology that uses both mating and mutation to create better chromosomes was pioneered by John Holland around the mid 1960's (Holland 2005). Since then, GAs have been used for a wide range of applications where an optimized solution with a large number of parameters is required.

Chromosomes that represent valid hypothesis need to be encoded as streams of data that can be processed by the algorithm. A pool of such encodings is referred to as the population and the GA progresses by updating this set of solutions. In each generation, new individuals are created randomly or through genetic operators such as crossover and mutation that recombine or mutate parent chromosomes respectively. Parent hypothesis from which offsprings are created, are selected according to a probability function.

In each generation step, all solutions are ranked by a fitness function and the population is updated to include the best individuals. The process is repeated until the algorithm stalls and no improvement in the fitness is detected with further processing. In this work, each chromosome represented a configuration and stored the dish locations.

As discussed by Mitchell (1997), GAs search through a large space to find the solution that maximises the fitness function. With the adopted approach, the algorithm is less likely to converge towards a local minimum since the operators can replace parent encodings with completely different offsprings. As the algorithm progresses, one must make sure that a group of good and similar encodings will not replicate and dominate the population.

3 CONFIGURATION

The specification document for phase 1 SKA specifies that 250 parabolic dishes each 15m in diameter will be installed over a 100km radius region (Dewdney 2010). 125 core stations (50%) will be fixed in the central 500m radius. The inner region and middle region will extend over a radius of 2,500m and 100,000m and will contain 50 (20%) and 75 (30%) antennas respectively. Figure 1 shows this layout.

In this study, a search for the optimum configuration that maximises the uniformity of the UV density distribution while keeping the connecting wire length to a minimum was conducted. The goal is to position the dishes in such a way as to obtain a flat uv distribution with points spread uniformly across the uv-plane (Cohanin 2004). A regular gridded mask representing the domain over which the dishes can be positioned, was initially generated. The initial encodings with possible configurations were then created with antenna locations chosen randomly from such a

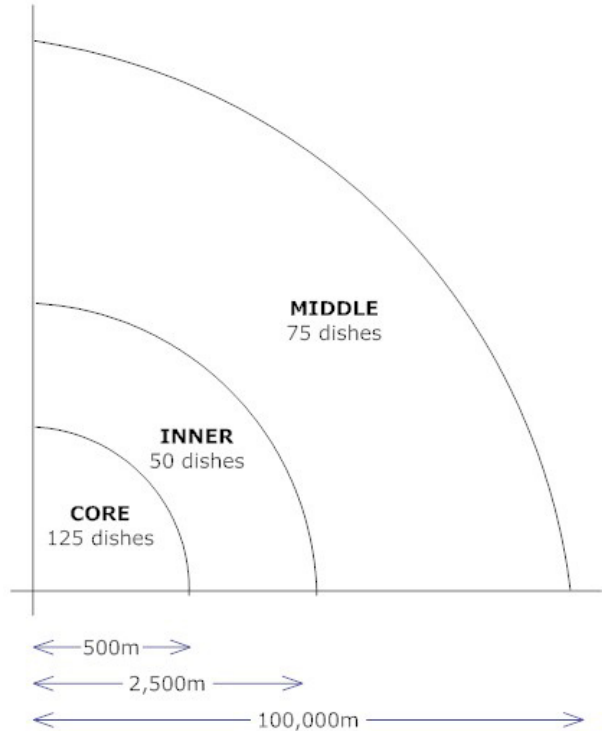


Figure 1. SKA phase 1 dish layout.

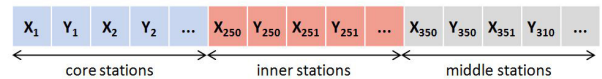


Figure 2. Dish configuration chromosome structure.

grid. The algorithm was let to evolve for a number of generations until no improvement in the fitness was detected and all encodings in the final population were similar. Due to the required number of dishes and receiver distribution, the initial population could not be biased with previously known good encodings.

3.1 Chromosome structure and genetic operators

Encodings that represented different configurations were created each one storing the x and y coordinates of the dish locations. As shown in Figure 2, each chromosome stored the mapping of dishes on the domain grid as a series of 500 integers. An identification number was also associated and stored with each encoding. This allowed the properties and status of each chromosome to be monitored and saved.

The crossover operation was designed to produce offsprings whose genes encode combinations of the core, inner and middle region. From every pair of parent chromosomes, after all gene combinations have been carried out, six new individuals were created. If the core, inner and middle regions of the first parent were represented by C1 I1 M1, and the second parent was made from C2 I2 M2, encodings with C1 I2 M1, C1 I1 M2, C1 I2 M2, C2 I1 M1, C2 I1 M2 and C2 I1 M1 were generated. To create more offspring by combining existing chromosomes, two more encodings were generated according to a randomly generated binary vector. In partic-

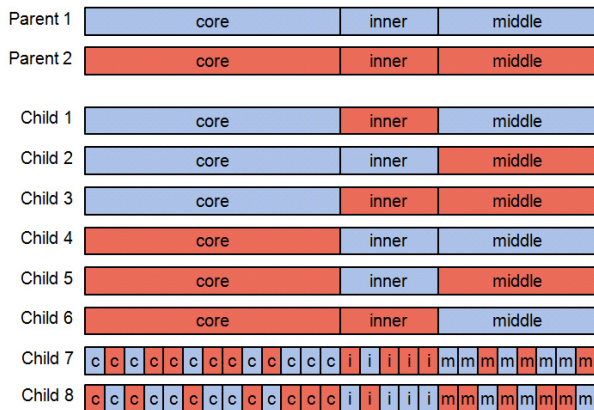


Figure 3. Offsprings created by the dish configuration crossover operator.

ular, dish positions corresponding to one were taken from the first parent while positions corresponding to zero were taken from the second parent. The binary vector was then bitwise inverted and the same procedure was repeated to obtain one more configuration. Since parent chromosomes may have common dish locations, the last two generated offsprings were checked by a gene repair function to ensure that all 250 locations were distinct. This crossover process is graphically shown in Figure 3.

The mutation operator was implemented such as to alter the positions of randomly selected dish locations. This allowed the algorithm to keep searching and to consider closely related encodings in the multidimensional search space. Although most parts of the chromosomes remained unchanged after mutation, the shifting of some of the dishes to a new location prevented the algorithm from converging onto a local maximum. In particular, a vector with 250 random values between 0 and 1 was populated. Indices of locations to which a number less than 0.2 was assigned were identified and new dish locations to the corresponding positions were determined. Chromosomes created by mutation were processed by the gene repair function to ensure that no location had more than one dish assigned to it.

3.2 Fitness functions

3.2.1 UV density distribution fitness

In order to ensure that the genetic algorithm converged towards a solution that maximised UV coverage, the density map was computed from every unique pair of dishes by equation 1.

$$\begin{pmatrix} u_{i,j} \\ v_{i,j} \\ w_{i,j} \end{pmatrix} = \frac{1}{\lambda} \begin{pmatrix} x_i - x_j \\ y_i - y_j \\ z_i - z_j \end{pmatrix} \quad (1)$$

Due to the nature of the dish array, $N(N-1)/2$ number of unique points (where N is the number of dishes) were generated. In certain test cases, the full coverage of the telescope after taking into consideration the rotation of the earth was also computed. As discussed by Segransan (2007), such pro-

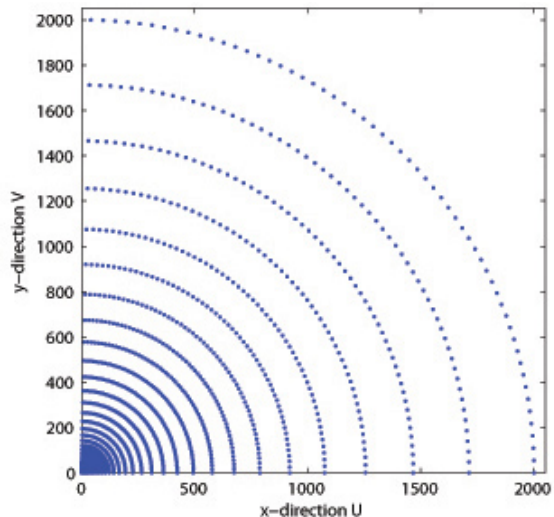


Figure 4. UV nominal grid quadrant.

jection can be determined by equation 2. Here, h represents the hour angle and δ is the source declination.

In order to be able to compare the resulting outputs, in this work the declination was always set to 90° to represent a radio object at the celestial north pole while the hour angle was set to range from 0° to 345° at 15° intervals.

Since the computation of the distance between all baselines becomes prohibitively expensive very quickly, we followed the work published by Cohanin (2004) and Cohanin et al. (2004). In particular, the nominal grid point closest to each UV point was determined and flagged. An analysis of the non-matched nominal points gave an indication of the distribution of the configuration and hence a measure of fitness. Ideally, the majority of nominal grid points would be flagged by at least one UV point.

Due to its size and current vision, the SKA will be a log based structure. As shown in Figure 4, a log distribution for the nominal grid was decided to be used. The goal of the GA was then set to minimise the fitness function, i.e. the percentage of non-matched nominal grid points. As in Cohanin et al. (2004), these were calculated using equation 3.

$$f_{UV} = \frac{N_{total} - N_{matched}}{N_{total}} \quad (3)$$

Here, N_{total} is the total number of points in the nominal grid and $N_{matched}$ is the total number of matched points. The numerator equates to the percentage of grid points that were not matched with any UV point.

Fitness evaluation of every individual required an efficient calculation of the UV density distribution as well as the mapping onto the nominal grid for a large number of chromosomes. We selected to use a k-dimensional tree representation of the nominal grid which needed to be computed only once and could be then stored in memory. The nearest point to every position encoded could then be determined by traversing the constant binary tree data structure. Since the nominal grid was defined over two dimensions, each non-leaf node represented a perpendicular hyperplane that divided

$$\begin{pmatrix} u_{i,j} \\ v_{i,j} \\ w_{i,j} \end{pmatrix} = \frac{1}{\lambda} \begin{pmatrix} \sin(h) & \cos(h) & 0 \\ -\sin(\delta)\cos(h) & \sin(\delta)\sin(h) & \cos(\delta) \\ \cos(\delta)\cos(h) & -\cos(\delta)\sin(h) & \sin(\delta) \end{pmatrix} \begin{pmatrix} x_i - x_j \\ y_i - y_j \\ z_i - z_j \end{pmatrix} \quad (2)$$

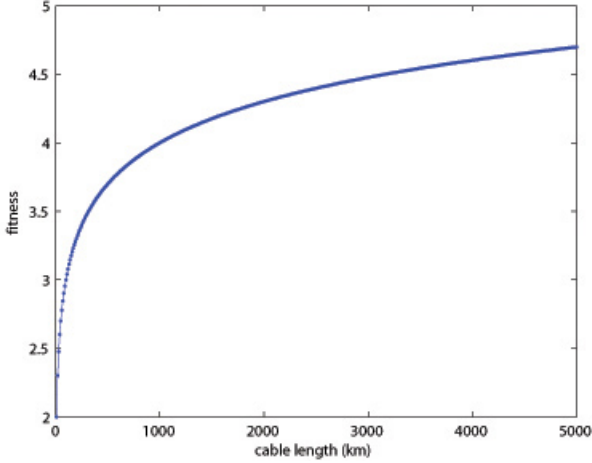


Figure 5. Log scale cable length fitness ($f_{WireLog}$).

the space into two subspaces. The left subtree pointed to other nodes on the left while the right subtree represented points to the right.

3.2.2 Logarithmic wire length fitness

Various approaches that attempt to compute an accurate cost and minimise the required length of cable to connect the dishes together, have been presented. Grigorescu et al. (2009) provide a set of algorithms that also take into account trenching, as well as connection costs to optimise a telescope layout infrastructure. In Cohanim et al. (2004), the single linkage algorithm is used. Here, to determine the shortest sequence that connects all vertices together, the Kruskal Minimum Spanning Tree (MST) algorithm (Cormen et al. 2001) was used.

Throughout this work, a cable with unit cost per unit length that connects all dishes in the core, inner and middle regions, was assumed. Dish locations were connected in such a way as to create an undirected graph in which edges (connections) between each vertex (dishes) had no particular direction. The weight of every edge was taken to correspond to the Euclidian distance between the two connecting nodes. The MST algorithm was then used.

Since the UV density fitness corresponds to a percentage ranging from 0 (optimum UV distribution) to 1 (worst case), a normalizing function that allows the computed wire length to be compared and added with the resulting UV fitness, was required. A log based approach was initially adopted and the cable length fitness was computed by equation 4.

$$f_{WireLog} = 1 - \log_{10} \left(\frac{1}{wirelength} \right) \quad (4)$$

The wire length is given in kilometers. Figure 5 shows the fitness values for cable lengths between 0 and 5000km.

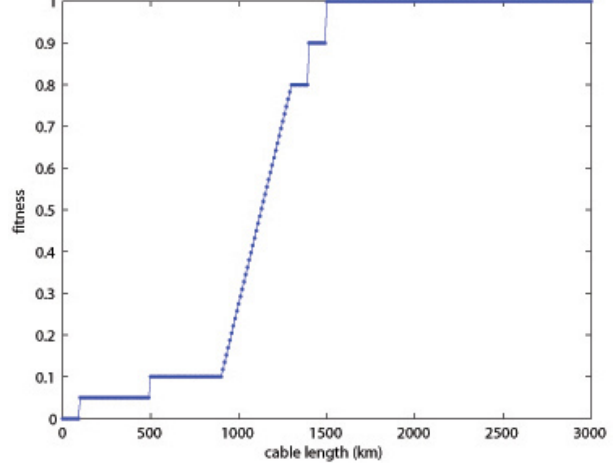


Figure 6. Stepwise cable length fitness ($f_{WireStep}$).

3.2.3 Stepwise wire length fitness

Since the majority of chromosomes were found to have a cable length of about 1000km, a stepwise function that linearly varies the output between 0.1 and 0.8 for wire lengths between 900km and 1300km was implemented. More specifically, the wire length fitness in this case was computed by equation 5.

$$f_{WireStep} = \begin{cases} 0 & \text{if } 0 \leq wirelength < 100; \\ 0.05 & \text{if } 100 \leq wirelength < 500; \\ 0.1 & \text{if } 500 \leq wirelength < 900; \\ 0.1 \rightarrow 0.8 & \text{if } 900 \leq wirelength < 1300; \\ 0.8 & \text{if } 1300 \leq wirelength < 1400; \\ 0.9 & \text{if } 1400 \leq wirelength < 1500; \\ 1 & \text{otherwise;} \end{cases} \quad (5)$$

In this way, the algorithm could accurately assign and rank individuals. Figure 6 depicts this stepwise variation with wire length more clearly.

3.2.4 Wire length penalty fitness

Further tests suggested that a wire length penalty approach may be more effective. Individuals encoding dish locations that could be connected by a cable length of less than 1250km, were not penalised. Chromosomes with a minimum wire length greater than 2250 were highly discouraged through a fitness assignment of 1. Intermediate cable lengths were given a weighting which varied linearly as described by equation 6. This variation of wire length fitness is presented in Figure 7. The threshold values used were determined after noting the results obtained in previous runs. The main advantage of this approach was that it directed the search towards solutions with a good UV coverage and penalized encodings that have a wire length above the norm. All en-

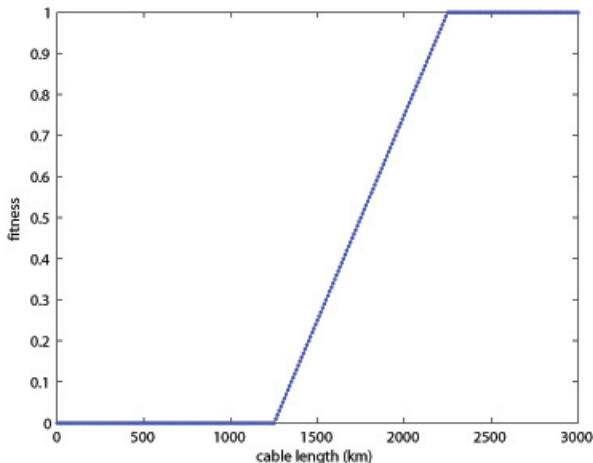


Figure 7. Penalty cable length fitness ($f_{WirePenalty}$).

codings with a cable length of less than 1250km were treated equally and the fitness was taken to depend solely on the UV distribution.

$$f_{WirePenalty} = \begin{cases} 0 & \text{if } 0 \leq wirelength < 1250; \\ 0 \rightarrow 1 & \text{if } 1250 \leq wirelength < 2250; \\ 1 & \text{otherwise;} \end{cases} \quad (6)$$

As discussed in subsequent sections, in order to compare the results obtained in this study with a generic configuration, dishes in the middle region were clustered together. This group formation naturally minimised the wire length and to account for these encodings, another wire penalty fitness function with lower thresholds was defined. This is formally defined by equation 7 below.

$$f_{WirePenaltyLow} = \begin{cases} 0 & \text{if } 0 \leq wirelength < 300; \\ 0 \rightarrow 1 & \text{if } 300 \leq wirelength < 450; \\ 1 & \text{otherwise;} \end{cases} \quad (7)$$

3.2.5 Power spectrum fitness

Any improvement gained through the introduction of power spectra calculation as part of the fitness function, was also investigated. Studies such as Parsons et al. (2011) provide detailed algorithms of how to compute power spectrum. However, for this study, work done by Green (2007) was followed to determine the raw angular power spectrum from the UV-plane. In particular, the number of UV points that coincided with log spaced annuli of width equal to the restricted zone diameter of the dishes, was determined. The resulting data series was divided by a log decaying curve and a mean value was computed to obtain a measure of fitness proportional to the distance between the two curves ($f_{PowerSpectrum}$). A typical raw angular power spectrum and the considered ideal curve are shown in Figure 8.

As the GA progressed, the fitness of individuals in each population were computed in parallel. The algorithm was left to evolve until it stalled and there was very limited im-

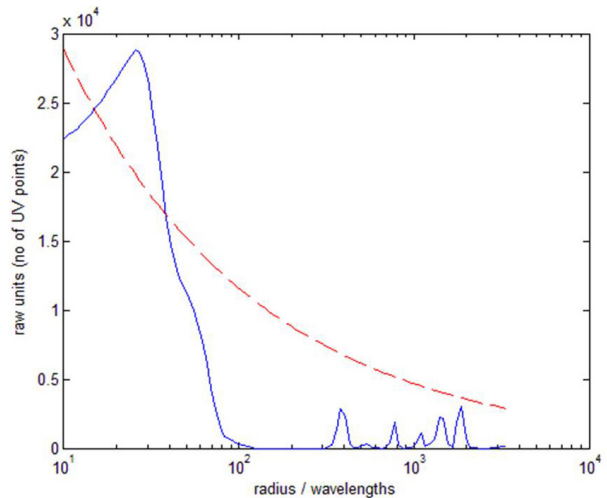


Figure 8. Raw angular power spectrum (blue) and a log decaying curve used as reference for fitness calculation (red).

provement with subsequent processing. As discussed in Section 4 below, runs using various combinations of the above mentioned fitness criteria were conducted.

4 RESULTS FOR SKA PHASE 1

An analysis of how the optimum configuration changes with different fitness functions, population sizes, and criteria for selecting individuals for subsequent generations, was carried out. In the following subsections the results obtained for different cases are presented.

4.1 Case 1 - GA with UV and log scaled wire length fitness

As a first test run, the genetic algorithm was set with an initial population of 1024 random chromosomes. For each individual, the overall fitness was calculated by equation 8.

$$f_{dish1} = f_{UV} + f_{WireLog} \quad (8)$$

Subsequent generations were created after selecting the fittest 1024 individuals from a pool of 4096 that consisted of 1024 chromosomes created by mutation, 2048 chromosomes created by crossover and 1024 new randomly generated chromosomes. The initial population had a mean and minimum fitness of 4.788 and 4.73 respectively. After 119 generations, the average fitness reduced to 4.421 and the most optimum individual had a fitness of 4.414. A plot of the resulting dish positions together with the computed wire length is presented as Figure 9. The corresponding mapping of the UV density distribution onto the nominal plane is shown in Figure 10.

4.2 Case 2 - GA with weighted UV and stepwise cable length fitness

In the second case, the UV coverage and wire length were given a weighting of 60% and 40% respectively as defined in

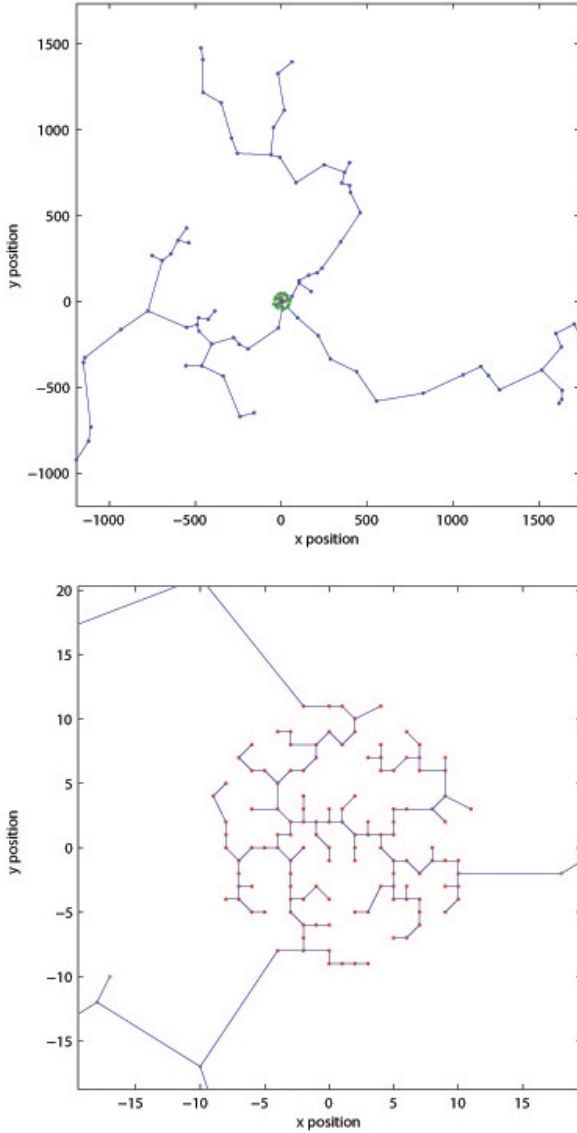


Figure 9. Full (top) and zoomed (bottom) dish configuration with shortest wire connecting the middle (blue), inner (green) and core (red) regions for Case 1.

equation 9. Experimenting with different weighting schemes allow the stakeholders to have a better understanding of the tradeoffs between performance and cost.

$$f_{dish2} = (0.6 \times f_{UV}) + (0.4 \times f_{WireStep}) \quad (9)$$

The initial population size was set to 1024. Individuals for subsequent populations were selected from a pool of 1024 chromosomes generated through mutation, 2048 offsprings generated by crossover and another 1024 random encodings. The highest ranking chromosomes were also considered for migration into the next population.

After the first few iterations, the percentage of randomly generated chromosome rapidly decreased to zero. The selection of individuals generated through mutation also decayed with time. The strongest genes were created through

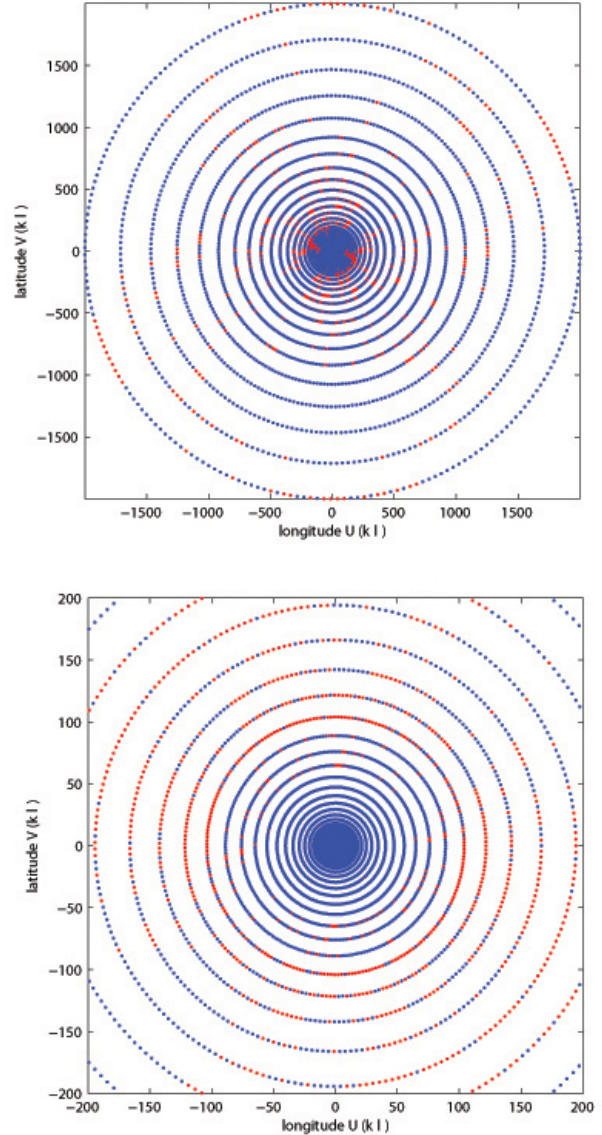


Figure 10. Mapping of the UV density distribution onto the nominal grid for the full array (top) and core region (bottom) showing the matched (blue) and unmatched (red) points for Case 1.

crossover and the algorithm converged after 111 iterations. Figure 11 shows the final dish locations and wire length while the UV distribution is presented in Figure 12. This had a UV density fitness of 0.67354 and wire length of 724.74km resulting in $f = (0.6 \times 0.67354) + (0.4 \times 0.1) = 0.4441$.

4.3 Case 3 - GA with UV and cable length penalty fitness

In this case, the input to the GA consisted of an initial population with 4096 chromosomes which encoded random positions for 250 dishes as defined in Section 3.1. At each step, parent chromosomes were selected from the population to generate 4096 new offsprings through mutation and another 8192 new individuals from crossover. The fitness of these

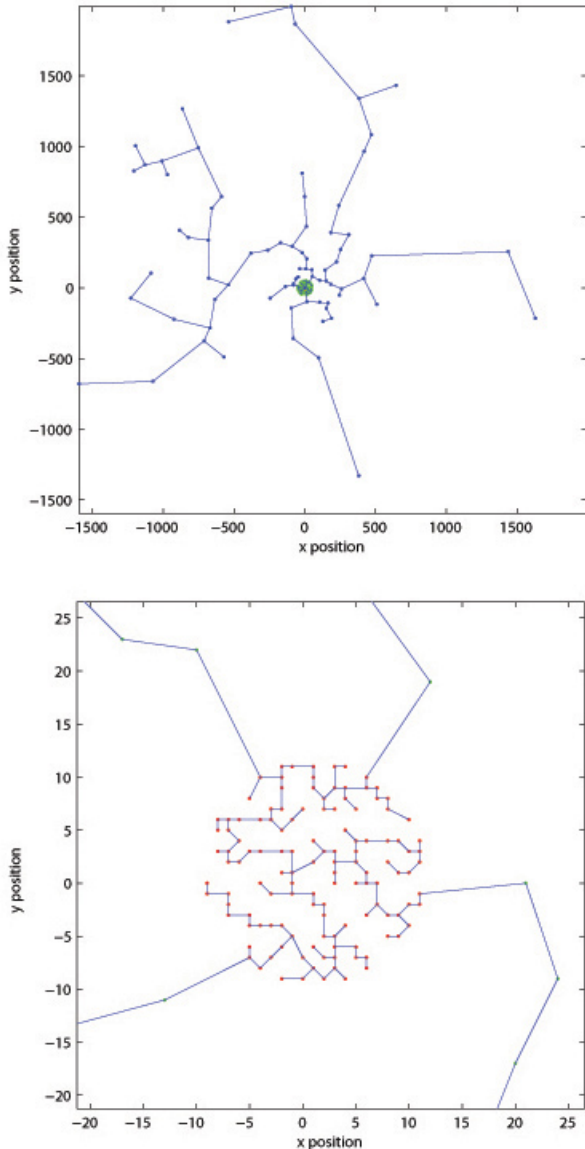


Figure 11. Full (top) and zoomed (bottom) dish configuration with shortest wire connecting the middle (blue), inner (green) and core (red) regions for Case 2.

new encodings as well as another 4096 randomly generated individuals were combined with the scores of the previous population and ranked to determine the fittest 4096 entries. These were selected for the next cycle and the process was restarted. In particular, the fitness was computed by equation 10.

$$f_{dish3} = f_{UV} + f_{WirePenalty} \quad (10)$$

Figure 13 gives an indication of the percentage of elite, crossover, mutation and random chromosomes selected at each generation. As expected, after the first few iterations, the genetic operators produced individuals with improved fitness and the algorithm progressed by continuously choosing offsprings generated through crossover. Randomly generated individuals became phased out and soon resulted

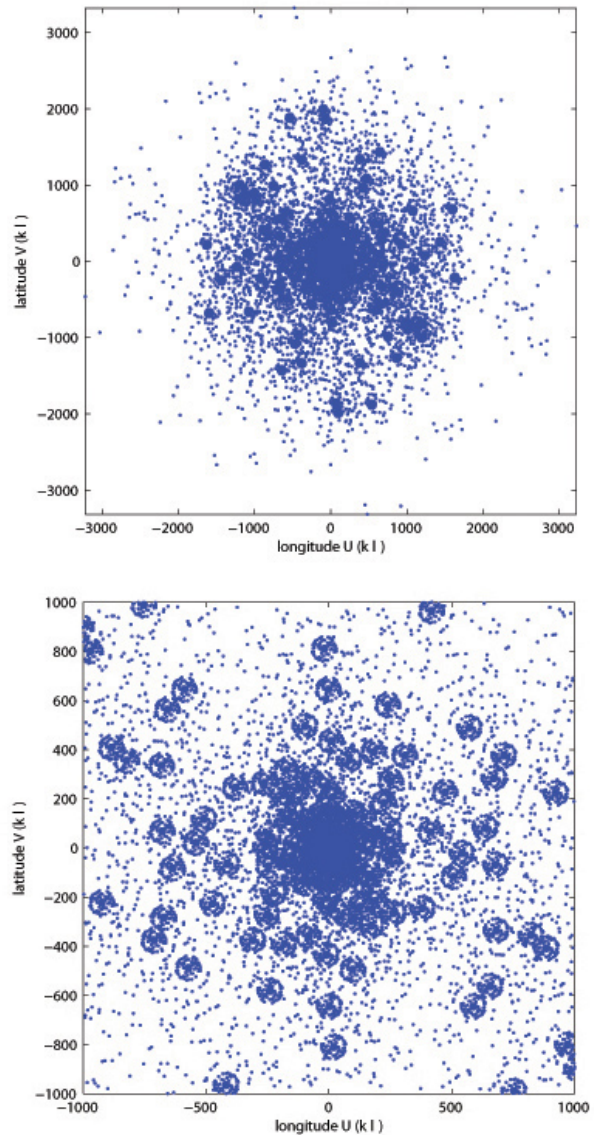


Figure 12. UV density distribution for the full array (top) and core region (bottom) for Case 2.

to have a lower fitness than the new offspring generated through the combination of chromosomes already in the population. Figure 14 shows the typical lifetime for crossover chromosomes, mutation chromosomes and randomly created individuals before they got replaced by fitter members. Encodings generated by the implemented genetic operators proved to have a longer lifetime than random chromosomes. This sped up the convergence of the algorithm as well as permitted the generation of fitter configurations.

Figure 15 shows how the fitness improved as the algorithm progressed. Figure 16 presents a rendering of the fittest encoding after 102 generations. Dishes in the middle, inner and core regions are shown in blue, green and red respectively. The UV density distribution percentage was 0.66825 while the minimum wire length computed by the MST algorithm was found to be 815.12km. Full and zoomed

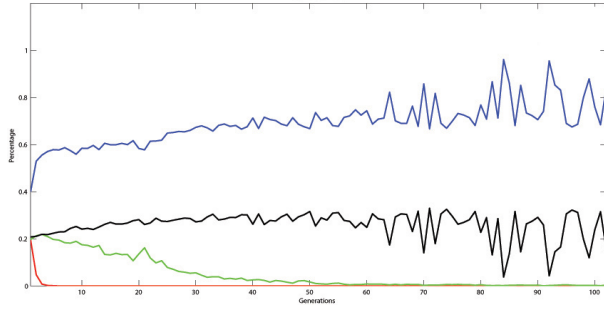


Figure 13. Percentage of elite (black), crossover (blue), mutation (green) and random (red) chromosomes selected for each population for Case 3.

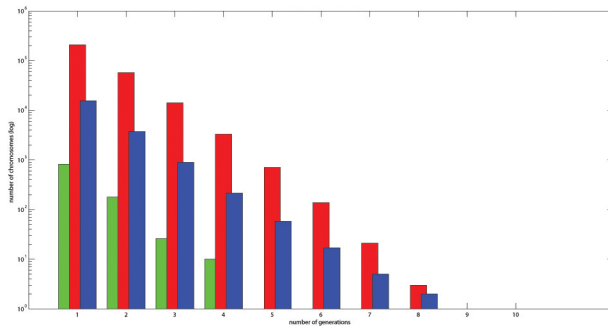


Figure 14. Lifetime of crossover (red), mutation (blue) and random (green) chromosomes for Case 3.

versions of the UV distribution calculated from all dish positions is presented in Figure 17.

4.4 Case 4 - GA considering randomly oriented grouped outer dishes with UV and cable length penalty fitness

In this case, the dish positioning and genetic functions were modified so that configurations had the elements in the middle region grouped in small random clusters of 3 to 8 dishes each. Elements were positioned in a circular, triangular or linear fashion and were given a random orientation. Since dishes were not randomly scattered, the required ca-

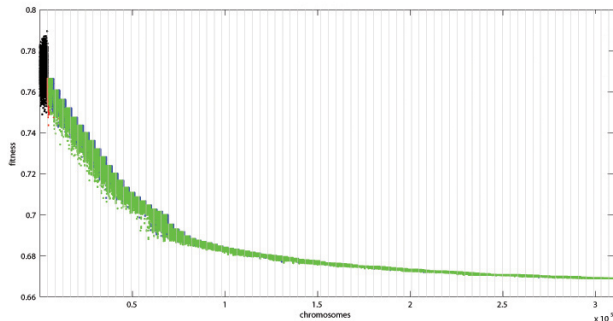


Figure 15. Fitness for the initial individuals (black), random chromosomes (red) and offsprings generated by the mutation (green) and crossover (blue) operators for Case 3.

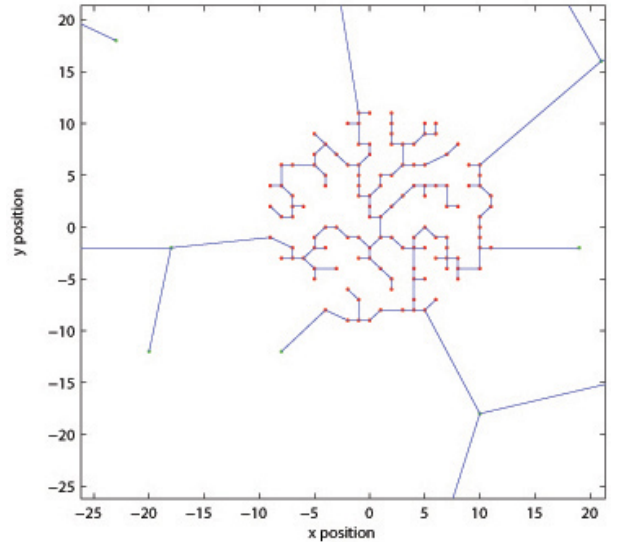
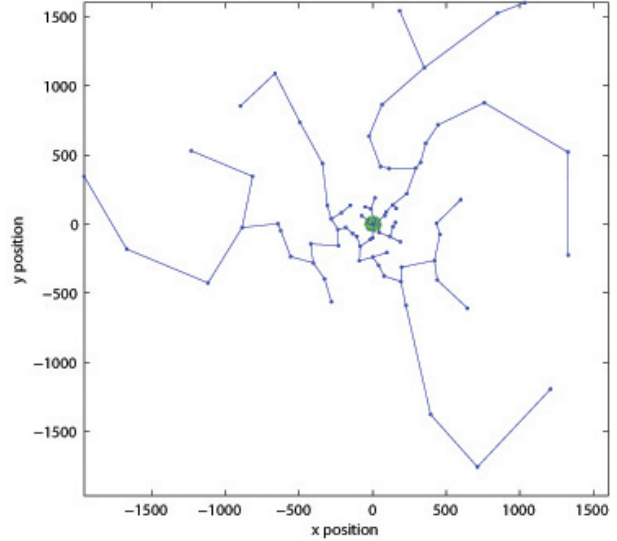


Figure 16. Full (top) and zoomed (bottom) dish configuration with shortest wire connecting the middle (blue), inner (green) and core (red) regions for Case 3.

ble length was expected to be less and the fitness function defined by equation 11 was used.

$$f_{dish4} = f_{UV} + f_{WirePenaltyLow} \quad (11)$$

The crossover function used in the previous cases could still be used since the middle region of all chromosomes had the exact same number of elements. Genes from any two parents could be swapped and still generate valid offsprings. However, the mutation operator had to be redefined. If a dish within the middle region was selected for mutation, a new position and shape for the entire group had now to be determined. Since each encoding could have a different number of groups with different number of dishes, further logic had to be performed before randomising the chromosome. Apart from the chromosome id, an integer with numerals that corresponded with the number of dishes in each group was also stored for each chromosome. Consecutive (x, y) co-

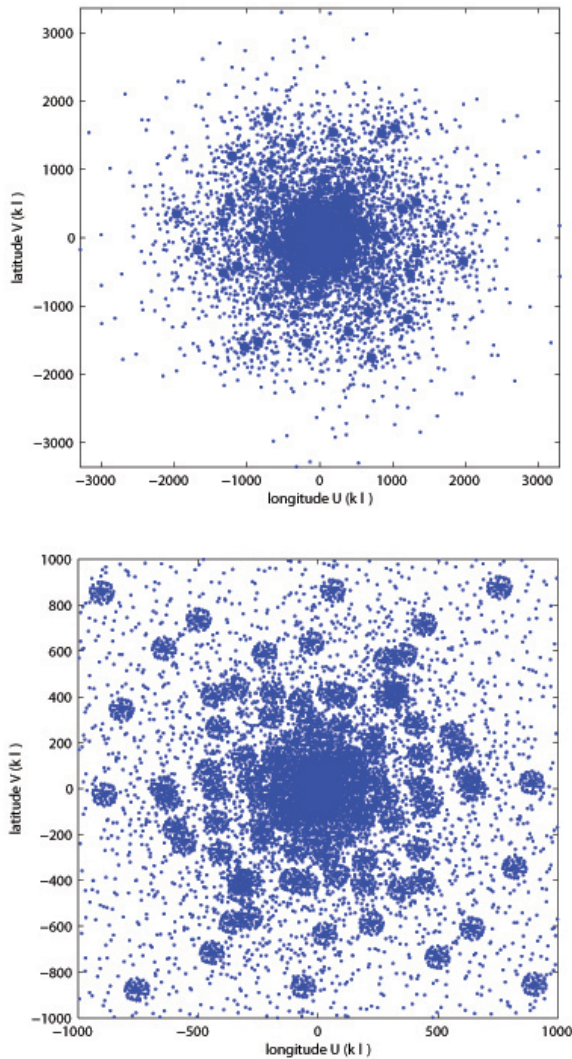


Figure 17. UV density distribution for the full array (top) and core region (bottom) for Case 3.

ordinates could then be read until the required group of stations was found.

Figure 18 and Figure 19 show the resulting configuration and the connecting wire respectively. Although the UV density distribution corresponds to a fitness of 0.77214 and a large number of nominal grid points are unmatched, the clustering of dishes allowed for a short cable length of 154.46km. For this run, the algorithm was made to work on a population of 1024 chromosomes and evolved for 102 generations before it stalled.

4.5 Case 5 - GA considering grouped outer dishes in a circular orientation with UV and cable length penalty fitness

Although dishes in the middle region were grouped as described for the previous case, clustered elements were now only positioned and oriented in a constant configuration. As shown in Figure 20, the corresponding UV distributions for dishes positioned in a straight line, in a triangle, as a

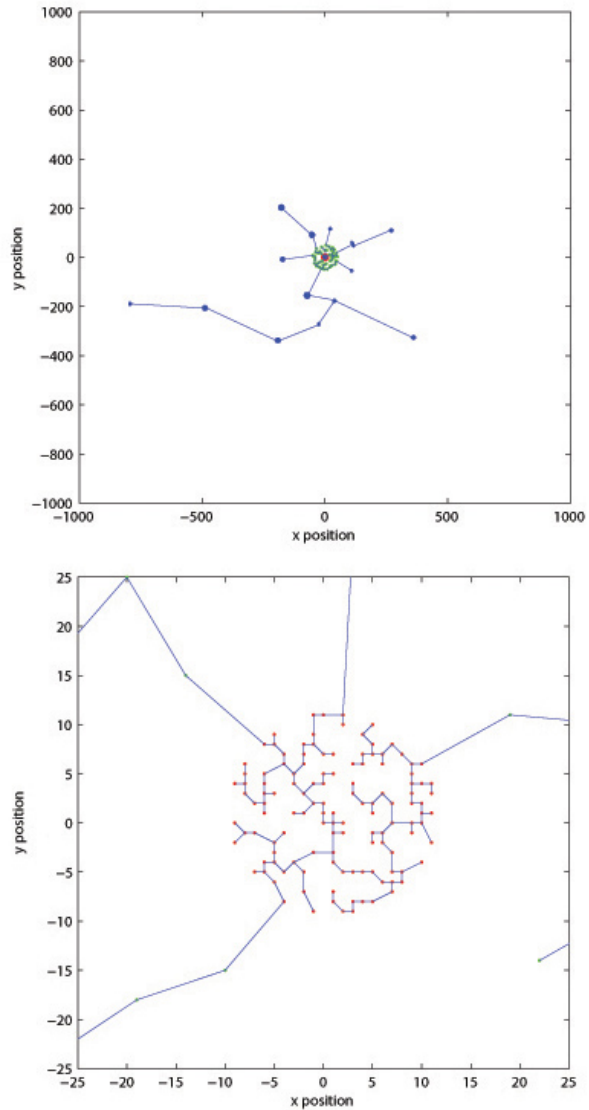


Figure 18. Full (top) and zoomed (bottom) dish configuration with shortest wire connecting the middle (blue), inner (green) and core (red) regions for Case 4.

snowflake, in a circular pattern and in a reuleaux triangle orientation, were initially determined. In each case, 29 to 30 elements were used to render well the required shapes. For a small number of elements, the configurations and the UV coverage of the circular and reuleaux orientations are very similar and the algorithm was set to distribute the dishes in the groups as such.

Figure 21 shows one of the resulting configurations after letting the GA run for 102 generations. The corresponding UV pattern and UV mapping onto the nominal grid are shown in Figure 22 while Figure 23 shows the constant decay in fitness with generations. Here the UV fitness and wire length resulted to be 0.777321 and 120.94km respectively.

To determine how the resolution improves with longer observation times, another run that takes into account the earth's rotation and which considers the UV projection over 24 hours, was performed. Due to the extra calculations involved, the fitness computation of each chromosome required

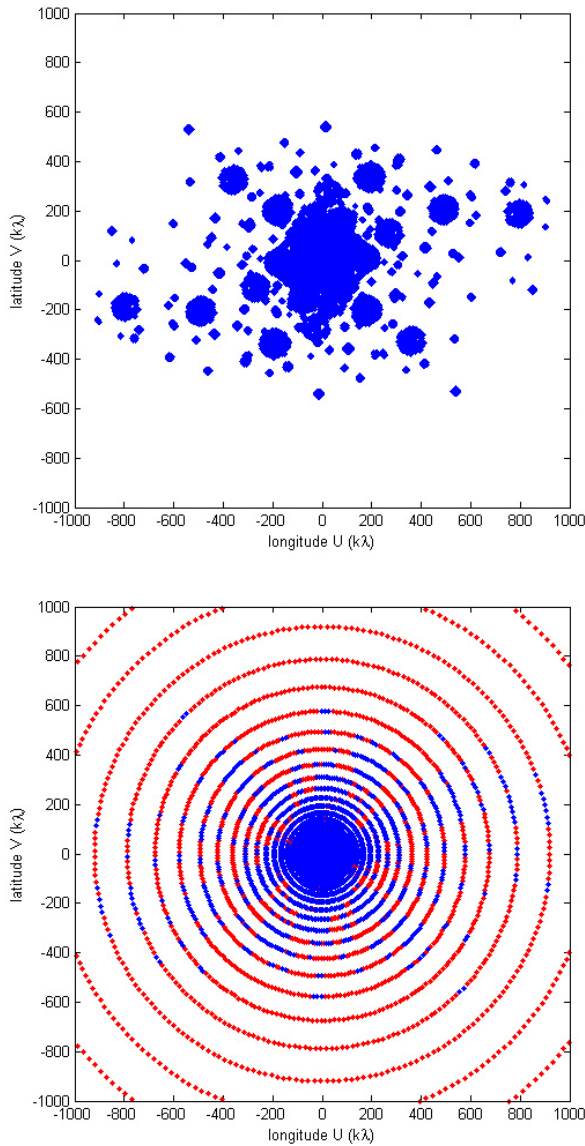


Figure 19. UV density distribution (top) and mapping onto the nominal grid (bottom) showing the matched (blue) and unmatched (red) points for Case 4.

on average 37.26 seconds. To finish processing in reasonable time, a population size of 128 was set. The resulting dish positions and the mapping of the UV points onto the nominal grid are presented in Figure 24 and Figure 25 respectively. As indicated by the shaded tracks, in this case the GA clearly chose a spiral configuration for the dishes in the middle region. Moreover, if the three arms are superimposed, the dishes would be roughly equally spaced along the track. The attained distribution is causing most of the nominal grid points to pair after a 360° rotation hence giving a very good UV fitness. The algorithm converged after 101 generations when a good compromise between UV density and cable length was found.

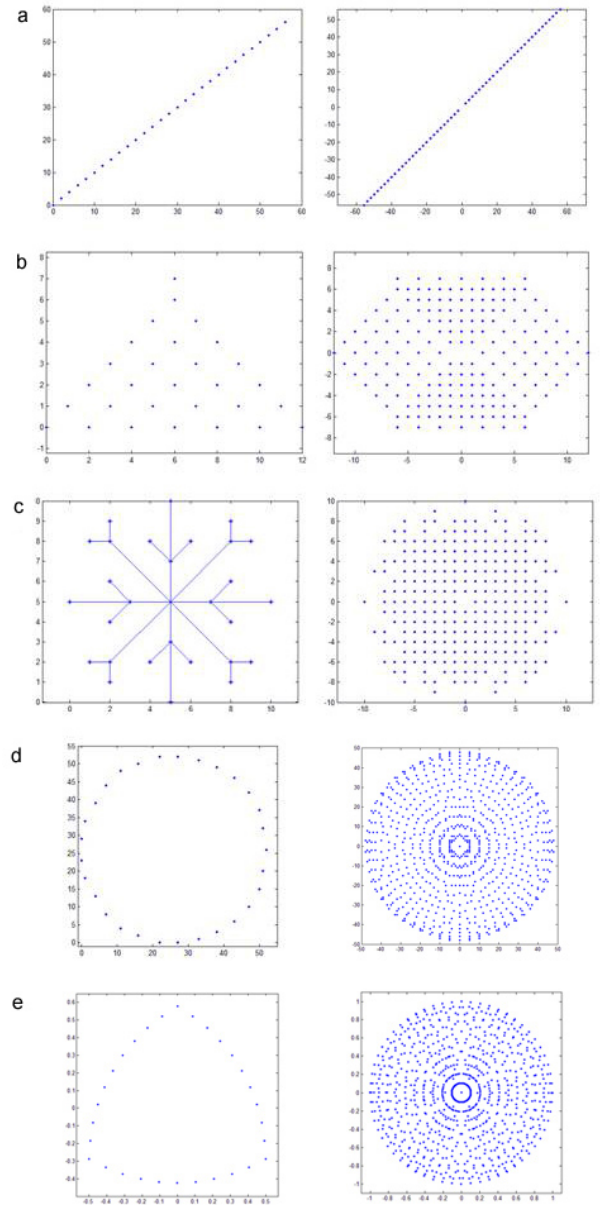


Figure 20. Orientation of 29 dishes (right) and the corresponding UV distribution (left) when placed in a straight line (a), triangle (b), snowflake (c), circular (d), and reuleaux triangle (e), configurations for Case 5.

4.6 Case 6 - Static SKA CTF and Reuleaux triangle configurations

Here, the fitness functions used in the other test cases were computed for static configurations. In particular, the generic configuration defined by the SKA Configurations Task Force (CTF) as well as a dish array specified by Reuleaux triangles were processed in order to be able to evaluate better the results achieved by GAs.

The generic dish configuration by the CTF is shown in Figure 26. The provided geographical coordinates were initially converted to cartesian points and projected onto the regular spatial grid considered in this work. The UV density distribution was then computed and mapped onto the

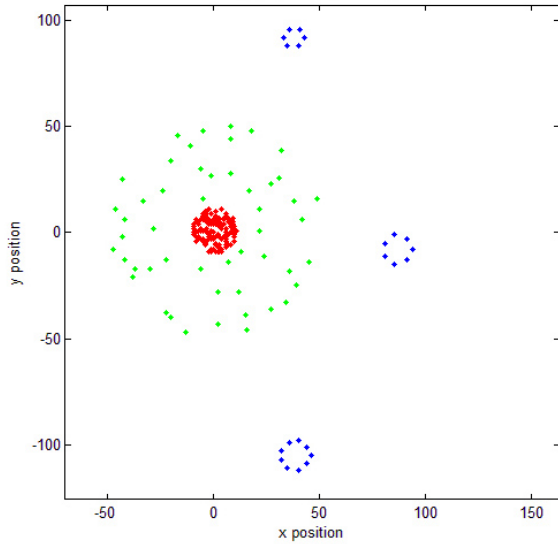
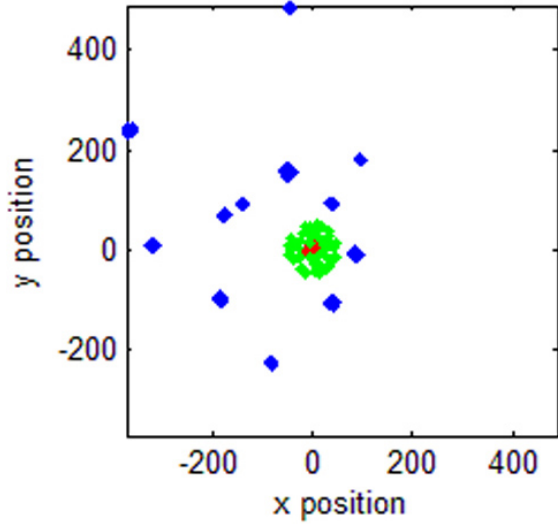


Figure 21. Full (top) and zoomed (bottom) dish configuration showing the middle (blue), inner (green) and core (red) regions for Case 5.

nominal grid to obtain the fitness measure f_{uv} . This was found to be 0.8093. The projection of the baseline vector on the sky over the period of one day was also considered and mapped onto the nominal grid. As expected this gave better coverage and reduced f_{uv} to 0.5243. Such a UV mapping is presented in Figure 27. The generic configuration was also processed by the MST algorithm which gave a wire length of 384.63km. The $f_{WireLog}$, $f_{WireStep}$, $f_{WirePenalty}$ and $f_{WirePenaltyLow}$ functions resulted to be 3.5850, 0.05, 0 and 0.5642 respectively.

After investigating the work by Keto (1997), a configuration defined with Releaux triangles was manually defined and tested. The dishes in the core were positioned over two slightly rotated triangles. Similarly, dishes in the inner region were placed according to a similar but larger shape. Receivers in the middle region were grouped but still positioned on randomly selected points from a predefined triangle. The UV fitness from the baseline vector (f_{uv}) was found to be 0.8234. However, when the 24 hour rotation of the earth

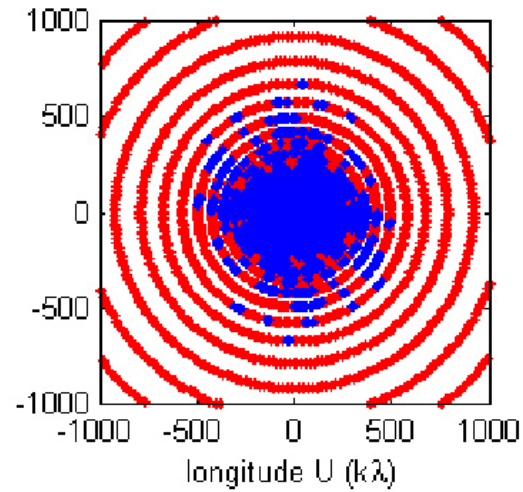
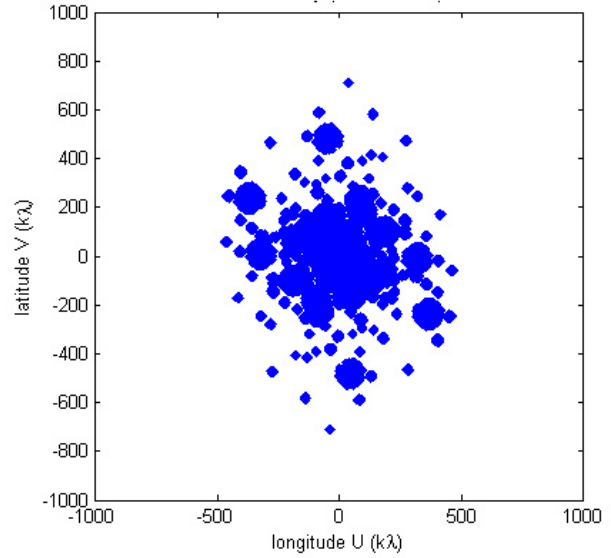


Figure 22. Mapping of the 24 hour UV density distribution onto the nominal grid for the full (top) and core region (bottom) showing the matched (blue) and unmatched (red) points for Case 5.

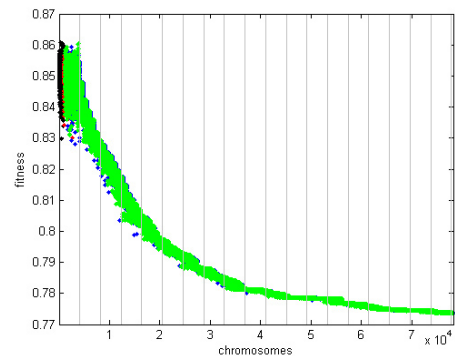


Figure 23. Fitness for the initial individuals (black), random chromosomes (red) and offsprings generated by the mutation (green) and crossover (blue) operators for Case 5.

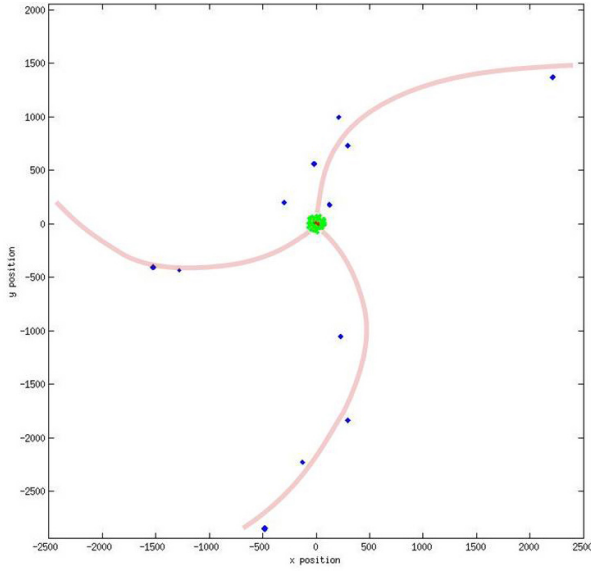


Figure 24. Dish configuration showing the middle (blue) and inner (green) regions with the spiral paths formed for Case 5 when considering a 24 hour projection.

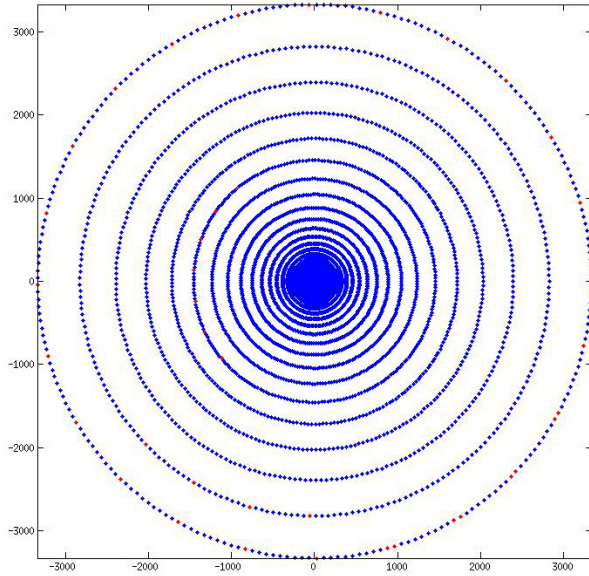


Figure 25. Mapping of the 24 hour UV density distribution onto the nominal grid showing the matched (blue) and unmatched (red) points for Case 5.

was taken into consideration, this improved to 0.6276. In both cases, the minimum cable length required to connect all dishes together was found to be 521.8439km. For this case, the $f_{WireLog}$, $f_{WireStep}$, $f_{WirePenalty}$ and $f_{WirePenaltyLow}$ functions equated to 3.7175, 0.1, 0 and 1 respectively. Figure 28 shows the defined configuration and the computed shortest wire for the core and inner regions.

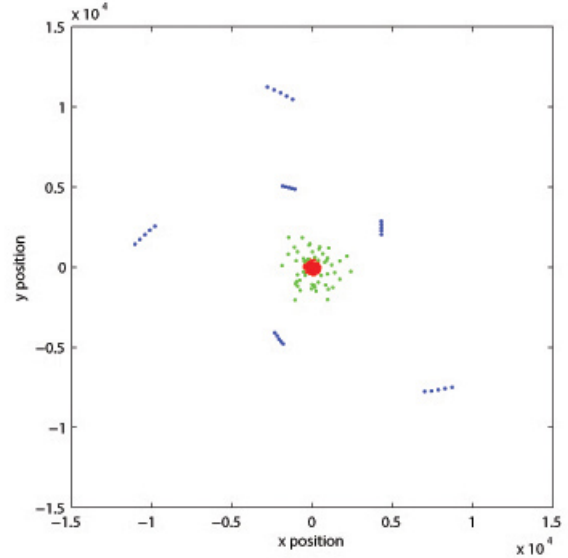
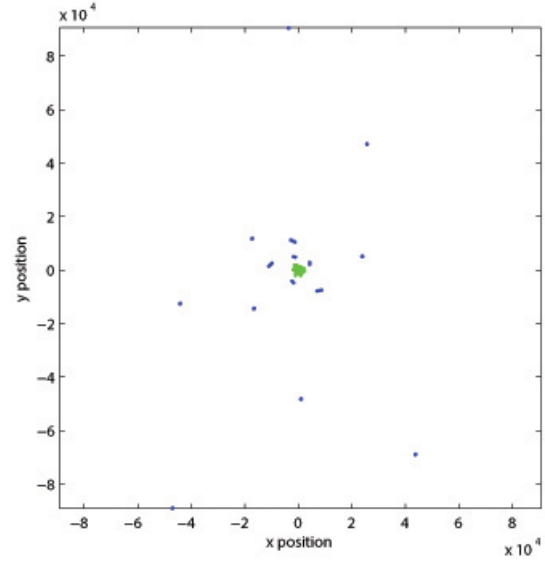


Figure 26. Generic SKA CTF dish configuration for Case 6.

4.7 Case 7 - GA with UV, cable length penalty and power spectrum fitness

To assess any improvements attained by adding the power spectrum to the fitness function, a test run with three parameters was set up. Individuals were ranked by equation 12.

$$f_{dish7} = f_{UV} + f_{WirePenaltyLow} + f_{PowerSpectrum} \quad (12)$$

In this case, the fitness evaluation function required a few more milliseconds to process each chromosome due to the extra calculations required for spectra computation. The GA still stalled after about 100 generations. However, a preferred configuration was determined after the first few iterates and as shown in Figure 29, no improvement was attained with subsequent processing. The chosen set of fitness criteria were not very compatible and hindered the genetic operators in creating fitter individuals. This can also be seen

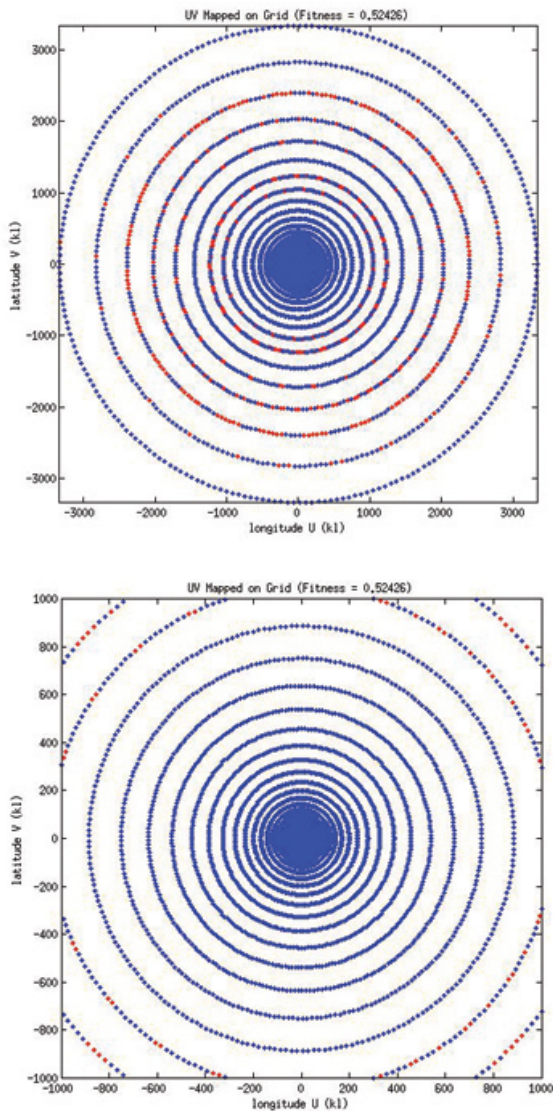


Figure 27. Mapping of the 24 hour UV density distribution onto the nominal grid for the full (top) and core region (bottom) of the CTF generic array showing the matched (blue) and unmatched (red) points for Case 6.

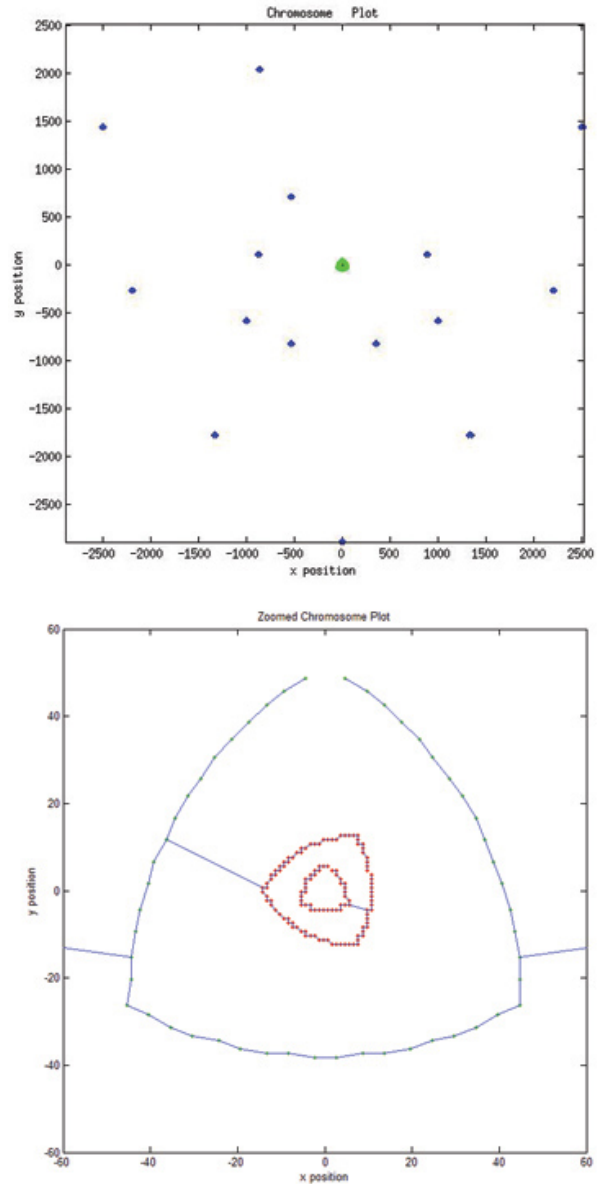


Figure 28. Full (top) and zoomed with shortest wire (bottom) dish configuration showing the middle (blue), inner (green) and core (red) regions for Case 6.

from Figure 31 in which constant migration of chromosomes from one generation to the next is evident. As can be seen from the UV mapping in Figure 30, the dishes in the outer region clustered together towards the edges and no other configurations were explored as the algorithm progressed.

The results obtained suggest that no significant improvement is gained after adding power spectrum estimation to the fitness function. In particular, the percentage of empty bins in the UV nominal grid corresponding to the fittest chromosome was found to be 0.8381%. The other test runs produced better results.

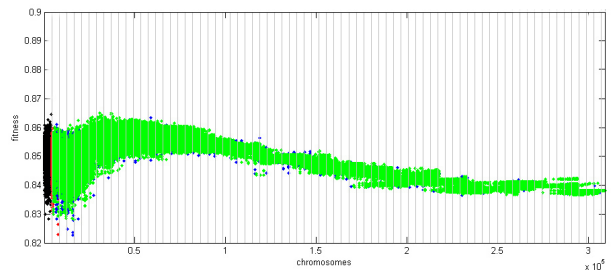


Figure 29. Fitness for the initial individuals (black), random chromosomes (red) and offsprings generated by the mutation (green) and crossover (blue) operators for Case 7.

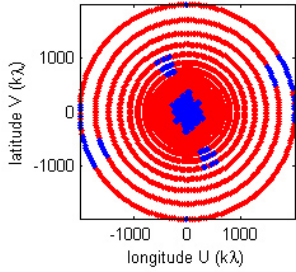


Figure 30. UV density distribution showing the matched (blue) and unmatched (red) points for Case 7.

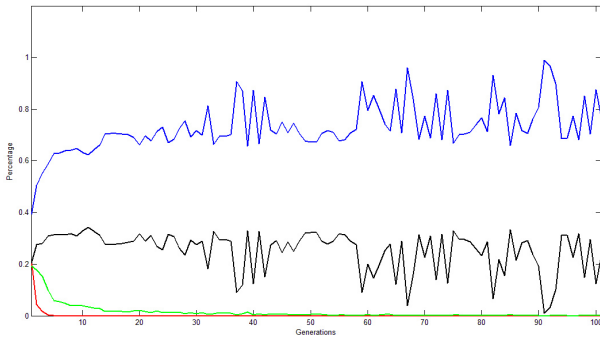


Figure 31. Percentage of elite (black), crossover (blue), mutation (green) and random (red) chromosomes selected for each population for Case 7.

5 RESULTS FOR SKA PHASE 2

Another genetic algorithm was programmed to search for an optimum dish configuration solution for SKA phase 2. As defined in Bolton et al. (2011), this will consist of 3000 dishes over a circular region of up to 3000km in radius. 600 dishes are to be positioned within the core area of 1km radius and 900 dishes will be installed up to a radius of 5km from the center. Another 900 and 600 dishes will be set up in the intermediate and outer regions which are planned to be limited to a 180km and 3000km radius respectively. Individual dishes will be positioned up to 13km from the center. Receivers located further away will be grouped. In this work, the intermediate region was set to contain 350 individual dishes and 50 stations with 11 dishes each. 25 stations of 24 dishes were set for the outer region. Figure 32 presents such a dish layout.

Dishes forming part of a group were positioned randomly in a station whose diameter was considered to vary depending on its distance from the central core. Specifically, the group radius (R_g) was made to vary as defined by equation 13.

$$R_g = \sqrt{\frac{\log(R) \times A \times N}{\pi}} \quad (13)$$

where R is the distance from the central core, A is the area occupied per dish given by $(\pi \times \text{RestZoneRadius})^2$ and N is the number of antennas.

Although the same chromosome structure as that shown in Figure 2 was used, all genetic operators and fitness functions had to be redefined due to the different number of

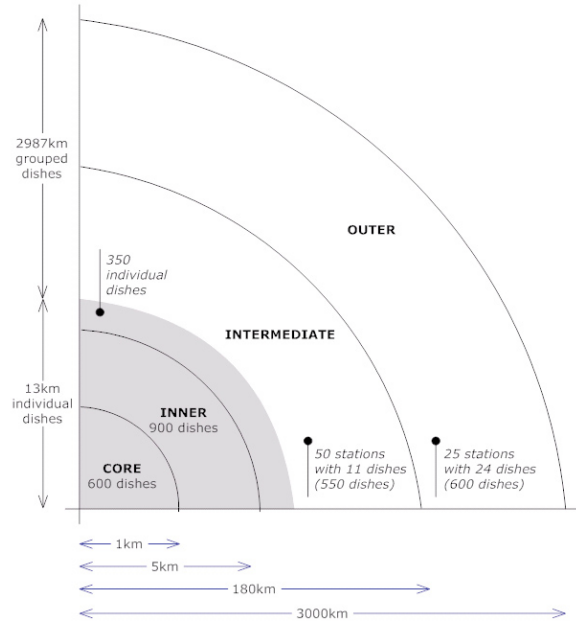


Figure 32. SKA Phase 2 dish layout.

dishes and regions. In order to be able to process and rank the required number of individuals in adequate time, some assumptions were made. Dishes in a station were treated as a single point for UV density calculation. The resulting points were also divided and mapped onto the nominal grid in parallel. Separate distance matrices and MSTs were computed for the main regions in order to obtain an approximate minimum wire length in the shortest time possible. The f_{dish3} fitness function was used.

Figure 33 shows the wire connecting the stations in the outer area. Connections between dishes inside a station are considered negligible. Figure 34 presents a zoomed plot of the individual dish locations in the core, inner and intermediate regions. The resulting UV density plot for the outermost stations is shown in Figure 35. Figure 36 gives the percentages of chromosomes that were generated through crossover, mutation, randomly or else that migrated from one population to the next (elite). In this case, the algorithm evolved for 101 generations before stalling.

6 CONCLUSION

In this work, we have investigated the use of genetic algorithms to determine the optimal configuration for the 250 dishes planned in phase 1 of the SKA telescope as well as for the 3000 dishes planned for phase 2. The uniformity of uv-distribution and the connecting wire length were used as parameters for optimisation. The affects of different dish orientations on the power spectrum, were also researched.

A number of test cases aimed to investigate different fitness functions and parameters, were presented. In all experiments, large genetic population sizes were used as much as possible. Although an upper limit of 250 was set to the number of generations, the processes always stalled prior to this and were stopped when no significant improvement in

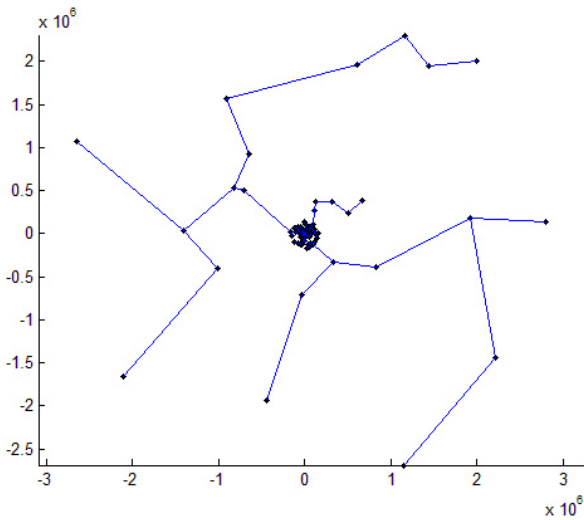


Figure 33. Connecting wire for the SKA Phase 2 stations in the outer region.

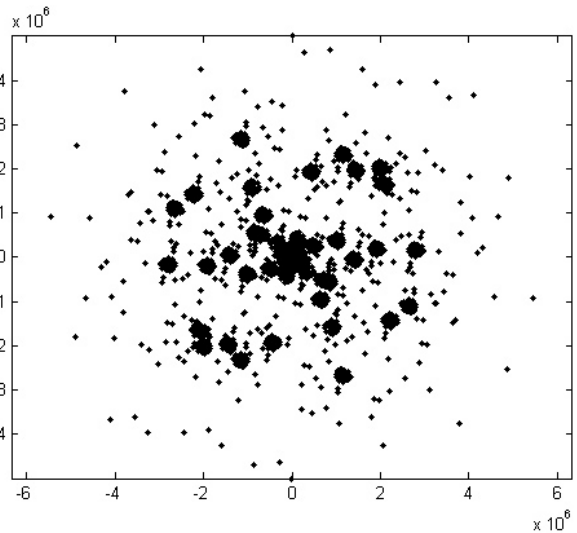


Figure 35. UV density distribution for the SKA phase 2 Dishes).

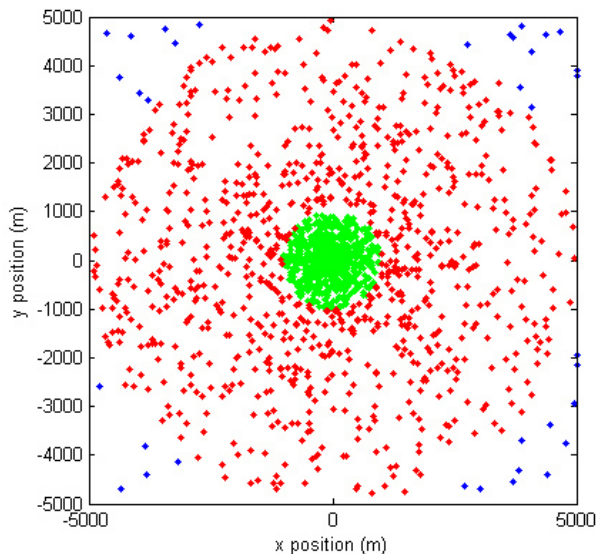


Figure 34. Positioning of the SKA Phase 2 dishes in the core (green) and inner (red) regions. A few receivers in the intermediate (blue) region can also be seen.

fitness was detected with subsequent iterations. In particular, the algorithms always converged between the 100th and the 120th iterate. The time taken for each run depended mostly on the fitness functions used. These were specifically implemented to run in parallel and allowed large population sizes to be set.

A summary of the results obtained in the test cases considered is presented in Figure 37. Although, the grouping of the stations in the middle layer improved the wire length fitness, this had a negative affect on the UV distribution criterion. The $f_{WirePenaltyLow}$ function was introduced to rank the individuals correctly even in such cases. This favored chromosomes that encoded a good tradeoff between UV coverage and cable length. As expected, better UV sam-

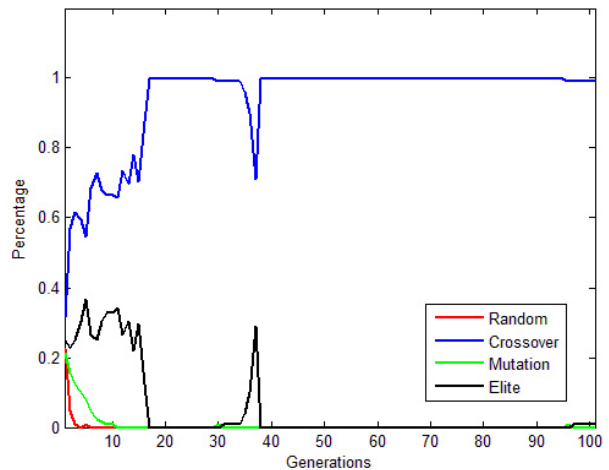


Figure 36. Percentage of elite (black), crossover (blue), mutation (green) and random (red) chromosomes selected for each population in the SKA Phase 2 run.

pling was obtained when 24 hour projections were considered.

Through this and similar work, the potential of machine learning techniques to aid in identifying optimal dish configurations was demonstrated. Promising results were obtained and further analysis can be done once more detailed specifications on the SKA are made available. For phase 2, the fitness functions had to be slightly modified and may need to be redefined as the number of dishes and domain area increase. The work done by Bounova and deWeck (2005) which describes an optimized framework to model robust and scalable networks, may also be considered to derive the best configuration for the full SKA.

Future work should also include a more detailed analysis of the affects of the power spectrum as well as other fitness measures.

Case	f_{UV}	Minimum wire length	$f_{WireLog}$	$f_{WireStep}$	$f_{WirePenalty}$	$f_{WirePenaltyLow}$	$f_{PowerSpectrum}$	Fitness Function	Fitness Value
SKA Phase 1 Case 1 GA with UV and log scaled wire length fitness	0.7199	494.7321	3.6944	0.05	0	1	n/a	f_{dish1}	4.4140
SKA Phase 1 Case 2 GA with weighted UV and stepwise cable length fitness	0.6735	724.7400	3.8602	0.10	0	1	n/a	f_{dish2}	0.4441
SKA Phase 1 Case 3 GA with UV and cable length penalty fitness	0.6683	815.1200	3.9112	0.10	0	1	n/a	f_{dish3}	0.6683
SKA Phase 1 Case 4 GA considering randomly oriented grouped outer dishes with UV and cable length penalty fitness	0.7721	154.4600	3.1888	0.05	0	0	n/a	f_{dish4}	0.7721
SKA Phase 1 Case 5a GA considering grouped outer dishes in a circular orientation with UV and cable length penalty fitness	0.7773	120.9400	3.0826	0.05	0	0	n/a	f_{dish4}	0.7773
SKA Phase 1 Case 5b GA considering grouped outer dishes in a circular orientation with UV and cable length penalty fitness (day projection)	0.5066	275.1504	3.4396	0.05	0	0	n/a	f_{dish4}	0.5066
SKA Phase 1 Case 6a Static SKA CTF	0.8093	384.6300	3.5850	0.05	0	0.5642	n/a	n/a	n/a
SKA Phase 1 Case 6b Static SKA CTF (day projection)	0.5243	384.6300	3.5850	0.05	0	0.5642	n/a	n/a	n/a
SKA Phase 1 Case 6c Static Reuleaux triangle configuration	0.8234	521.8439	3.7175	0.10	0	1	n/a	n/a	n/a
SKA Phase 1 Case 6d Static Reuleaux triangle configuration (day projection)	0.6276	521.8439	3.7175	0.10	0	1	n/a	n/a	n/a
SKA Phase 1 Case 7 GA with UV, cable length penalty and power spectrum fitness	0.8381	285.9274	3.4563	0.05	0	0	0.3474	f_{dish7}	1.1855
SKA Phase 2	0.1250	20654.0000	5.3150	1	1	1	n/a	f_{dish3}	1.125

Figure 37. Results for the SKA Phase 1 and SKA Phase 2 case studies.

7 ACKNOWLEDGEMENTS

The authors would like to express their deepest gratitude to Dr Eric R. Keto for his valuable comments and feedback. His expertise, guidance and support not only helped to improve this research but have inspired new ideas for other future work.

The analysis carried out would have not been possible if not for the computing power made available by the Department of Physics within the University of Oxford (UK) and the Physics Department within the University of Malta (Malta).

REFERENCES

- R. Bolton, R. P. Millenaar, and G. D. Harris. Ska configurations design, 2011. URL http://www.skatelescope.org/public/2011-02_System_delta_CoDR_Documents/18-WP3-050.020.000-R-002-A_SKAConfigurations.pdf.
- G. Bounova and O. deWeck. Graph-theoretical considerations in the design of complex engineering systems for robustness and scalability. Master's thesis, Massachusetts Institute of Technology, 2005.
- B. E. Cohanin. Multiobjective optimization of a radio telescope array with site constraints. Master's thesis, Massachusetts Institute of Technology, 2004.
- B. E. Cohanin, J. N. Hewitt, and O. Weck. The design of radio telescope array configurations using multiobjective optimization: Imaging performance versus cable length. *The Astrophysical Journal*, 154:705–719, 2004.
- T. H. Cormen, C. E. Leiserson, R. L. Rivest, and C. Stein. *Introduction to Algorithms*. McGraw-Hill, 2001.
- P. Dewdney. Ska-phase 1: Preliminary system description and cost estimate. *SKA Memo 130*, 2010.
- M. A. Garrett, J. M. Cordes, D. deBoer, J. L. Jonas, S. Rawlings, and R. T. Schilizzi. A concept design for ska phase 1. *SKA Memo 125*, 2010.
- D. A. Green. Angular power spectra of galactic hi with the sbps, 2007. URL http://www.skads-eu.org/p/svt/svt_green.pdf.

- G. Grigorescu, P. Alexander, R. Bolton, and R. McCool. Cost-effective infrastructure in a multi-antenna telescope layout. *SKA Memo 121*, 2009.
- R. Hassan, B. E. Cohanin, O. de Weck, and G. Venter. A comparison of particle swarm optimization and the genetic algorithm. In *46th AIAA/ASME/ASCE/AHS/ASC Structures, Structural Dynamics and Materials Conference*, Austin, Texas, AIAA-2005-1897, April 18 - 25 2005.
- J. H. Holland. Genetic algorithms - computer programs that evolve in ways that resemble natural selection can solve complex problems even their creators do not fully understand, 2005. URL <http://www2.econ.iastate.edu/tesfatsi/holland.gaintro.htm>.
- E. Keto. The shapes of cross-correlation interferometers. *The Astrophysical Journal*, 475(2):843, 1997. URL <http://stacks.iop.org/0004-637X/475/i=2/a=843>.
- T. M. Mitchell. *Machine Learning*. McGraw-Hill, 1997.
- A. Parsons, M. McQuinn, D. Jacobs, J. Aguirre, and J. Pober. A sensitivity and array-configuration study for measuring the power spectrum of 21cm emission from reionization. *arXiv:1103.2135v1 [astro-ph.IM]*, 2011.
- D. Segransan. Observability and uv coverage. *New Astronomy Reviews*, 51(8-9):597 – 603, 2007.